Chapter 1
High Energy/High Repetition Rate Laser Pulses from Yb Based Solid State Oscillators with Cavity-Dumping and Regenerative Amplifiers

Moritz Emons, Guido Palmer, Marcel Schultze, Uwe Morgner, Hakan Sayinc, Dieter Wandt and Dietmar Kracht

Abstract Various scientific and industrial laser applications profit from the latest progress of directly diode pumped high-power femtosecond oscillators, in particular applications such as laser micromachining, nonlinear spectroscopy, or laser surgery. These oscillators provide pulse energies in the microjoule regime at 100 kHz to megahertz repetition rates, replacing complex and expensive chirped-pulse amplification (CPA) systems. Regarding power and energy scaling, Yb-doped materials are of great interest, offering the opportunity of high-power diode-pumping plus the generation of femtosecond pulses. In this article, we report on recent progress in the generation of femtosecond pulses with high energies either from oscillators or from regenerative amplifiers. In the first part of this chapter we discuss solid state oscillators with cavity-dumping and solitary pulse shaping followed by the concept of oscillators in the positive dispersion regime. The principle of thin-disk oscillator technology and its suitability for cavity-dumping is discussed, and the latest results from our two-crystal oscillator are presented, followed by some selected applications. In the second part of this chapter the progress of regenerative thin-disk amplifier technology will be discussed including latest results from thin-disks of potassium yttrium and lutetium monoclinic double tungstate oxide.

M. Emons (✉) · G. Palmer · M. Schultze · U. Morgner
Institut Für Quantenoptik, Leibniz Universität Hannover, Welfengarten 1, 30167 Hannover, Germany
e-mail: emons@iqo.uni-hannover.de

H. Sayinc · D. Wandt · D. Kracht
Laser Zentrum Hannover e.V, Hollerithallee 8, 30419 Hannover, Germany
e-mail: h.sayinc@lzh.de

S. Nolte et al. (eds.), *Ultrashort Pulse Laser Technology*,
Springer Series in Optical Sciences 195, DOI 10.1007/978-3-319-17659-8_1

1.1 Solid State Oscillators with Cavity-Dumping

In this section we report on passively mode-locked Ytterbium-based oscillators with MHz repetition rate cavity-dumping in different dispersion regimes allowing for the generation of microjoule pulses directly from a single oscillator. When the laser is operated in the solitary regime the current limit in energy scalability is given by the exceeding nonlinearity from several microjoules of intracavity pulse energy [1]. For even higher pulse energies it is necessary to either significantly reduce the nonlinear propagation length or to operate the oscillator with less peak power. The latter approach can be realized with the positive dispersion concept. The spectral bandwidth of the resulting positively chirped pulses is explicit broader than in the solitary regime [2], which allows for the generation of femtosecond pulses after external compression.

When starting to scale the pulse energy in femtosecond oscillators with cavity-dumping the simplest approach for the generation of pulse energies exceeding 1 μJ is based on a single bulk-crystal (see Fig. 1.1). The $KY(WO_4)_2$-crystal can either be directly pumped by a free emitting laser diode or a fiber-coupled laser diode with up to 30 W at 980 nm. Typical resonator lengths which have been realized yield repetition rates around 16–19 MHz.

This repetition rate already offers reasonably high pulse energies and makes electronic switching unproblematic. Electro-optical cavity-dumping is achieved by the combination of a Pockels-cell (electro-optical modulator with BBO-crystals) and a thin-film polarizer (TFP). This method is the same for all following cavity-

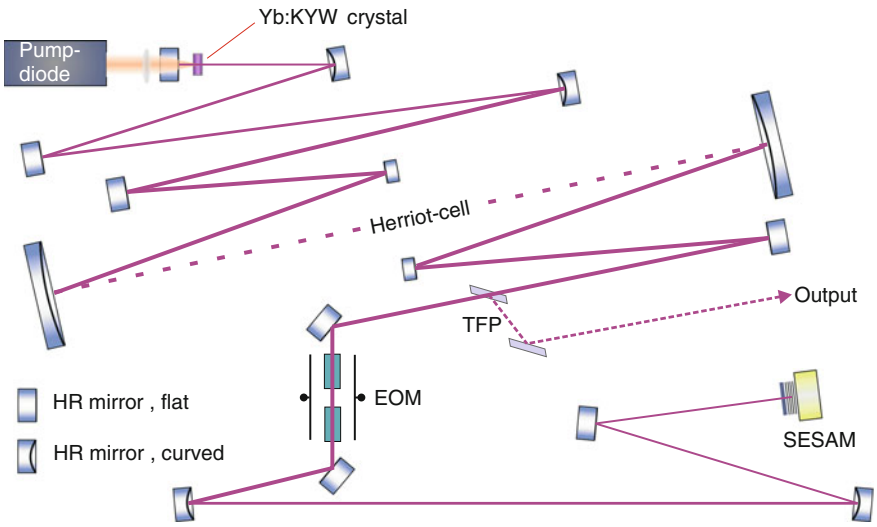

Fig. 1.1 Schematic of the laser setup, *EOM* electro-optical-modulator (BBO-Pockels-cell), *TFP* thin-film polarizer, *SESAM* semiconductor saturable absorber mirror, *Herriott-cell* number of reflections per mirror depends on cavity length (not shown)

dumped systems. The saturable absorber mirror stabilizes the solitary mode-locking against cw- and Q-switch-operation. Beside the N_m-optical axis (1030 nm) the bulk-laser can also be operated with polarization parallel to the N_p-optical axis at a wavelength of 1040 nm. The crystal length is between 1 and 2 mm with a typical Yb-doping concentration is of 5 at.%.

1.1.1 Solitary Regime in Bulk-Oscillators

For maximum internal pulse energies around 2.3 µJ a negative group-delay-dispersion of −9200 fs^2 is required to compensate for the nonlinearities (self-phase-modulation) in the solitary setup similar to that shown in Fig. 1.1 [2]. With cavity-dumping efficiencies of around 60 % the laser emits pulse energies of 1.35 µJ with pulse durations of 340 fs (time-bandwidth-product, TBP: 0.34). The attributed power spectrum is depicted in Fig. 1.2. The prominent sidebands are identified as Kelly sidebands from the perturbation of the soliton with the periodicity of the oscillator round trip frequency [3, 4].

Numerical simulations based on the soliton theory have led to a deep understanding of the pulse evolution and the dynamic behavior in the system [5]. They revealed that three dumping frequency regimes can be defined: the relaxation, the intermediate and the transient frequency regime for low (<20 kHz), medium and high (>80 kHz) dumping rates, respectively. For low repetition rates the time between the dumping is long compared to the period of the relaxation oscillations which allows the laser to relax to its steady state between two dumping events. In the 'intermediate' regime with a dumping rate close to the relaxation oscillation frequency (around 40 kHz), instability and subharmonic behavior is observed. At dumping frequencies higher than 80 kHz the laser has no time to relax before the

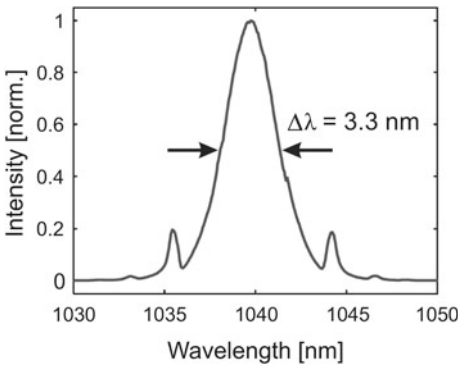

Fig. 1.2 Power spectrum of the solitary bulk laser clearly revealing Kelly sidebands which de-rive from the disturbance of the soliton-like pulses caused by the dumping. The laser was operated with polarization parallel to the N_p-optical axis resulting in a central wavelength of 1040 nm

next dumping occurs. The latter allows for dumping-frequencies from roughly 300 kHz to more than 1 MHz closing the gap between oscillators and solid-state amplifier systems [5].

1.1.2 The Chirped Pulse Oscillator (CPO)

For pulsed operation and a compact configuration the resonator was stretched to a total length of 8.64 m (repetition rate of 17.35 MHz) with a Herriott-type multipass cell (see Fig. 1.1). In contrast to the solitary regime a total material dispersion of +4250 fs^2 per round-trip for all participating optics was estimated. By changing type and number of the negative dispersive mirrors the magnitude of the net intracavity dispersion could be easily changed [6].

By using a SESAM stable self-starting cw-mode-locking operation of the laser has been achieved even though there is no pulse shaping mechanism from solitary pulse propagation. To sustain stability it was necessary to raise the pump power simultaneously while increasing the dumping ratio to compensate for the dumping losses. Stable mode-locking could be observed with dumping ratios up to 45 %. At that point the maximum output energy was beyond 2 μJ which is a factor of 1.4 higher compared to the solitary version from Sect. 1.1.1. We operated the oscillator in four different dispersion configurations, namely 250, 750, 1250 and 2250 fs^2 for the total GDD per round trip. The resulting power spectra are compared in Fig. 1.3 on a logarithmic scale. The distinctive rectangular shape is typical for chirped-pulse oscillators.

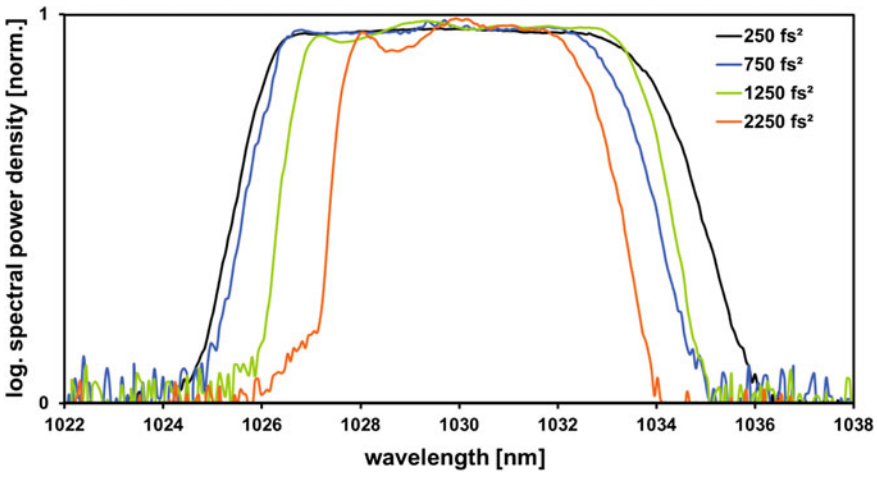

Fig. 1.3 Optical power spectrum of the output pulses for the different dispersion regimes

Beginning with a large dispersion of 2250 fs^2, the spectral bandwidth becomes significantly broader with decreasing net-dispersion, while the available output power remained constant for all four different dispersion values. The broadest bandwidth (FWHM) of 8 nm was observed at 250 fs^2. A further decrease of the GDD results in unstable pulsing. With a dispersion of 250 fs^2 the duration of the chirped output pulses was measured to be in the range of 3 ps (4.4 ps autocorrelation width). The measured rms-noise was below 1 % with a beam parameter M^2 of less than 1.1. The contrast ratio between the dumped pulses and the background exceeded 500:1.

Laser operation at 250 fs^2 is optimal when subsequent external pulse compression is used, since it provides the broadest spectrum enabling the shortest available pulse duration. In this case two fused silica transmission gratings with 1250 lines per millimeter were employed. The compressed pulses were analyzed with an intensity autocorrelator. By calculating the pulse duration directly from the power spectrum thus obtains a Fourier-limit of 360 fs (490 fs autocorrelation width). The measured autocorrelation reveals a FWHM of 570 fs resulting in a pulse duration of approximately 420 fs. The residual chirp led back to misalignments of the rather complex compression setup.

1.1.3 Thin-Disk Oscillator in the Solitary Regime

Using the previously discussed solitary mode-locked bulk oscillators (see Sect. 1.1.1) in combination with the cavity-dumping technique, a further scaling of the energy is limited by thermal effects and nonlinear contributions of the relatively long laser crystals. For this reason, the thin-disk concept is used instead to investigate the possibility for the generation of even higher pulse energies [1]. The thin-disk laser consists in principle of a very thin laser medium in combination with an optical multipass pump scheme. By using fibers for transport and homogenization of the pump light, low cost diode lasers can easily be coupled into the multipass pump system. Therefore the demands on brightness of the pumping diodes are comparably low. Due to the thin crystal, the homogeneous pump profile and the axial cooling geometry, such lasers are very resistant to thermal lensing [7, 8]. The schematic setup is similar to Fig. 1.1. The thin-disk acts as a folding mirror enabling four bounces per roundtrip. To maximize the absorbed pump power, a commercial thin-disk pump module is used which allows for 24 passes through the gain medium [9].

The 110 μm thin Yb:KYW disk is pumped with up to 50 W at 976 nm. Output coupling of the pulses is realized as before with a BBO-Pockels-cell in combination with a TFP. Mode-locking is induced by a SESAM with a modulation depth of approximately 1 % and a saturation fluence of about 90 $\mu J/cm^2$. Due to the high nonlinearity contributions from the Pockels-cell, the thin-disk and the ambient air, a total negative dispersion of 40,000 fs^2 is inserted into the cavity by means of dispersive mirrors (GTI) to fulfill the soliton condition. The maximum output power

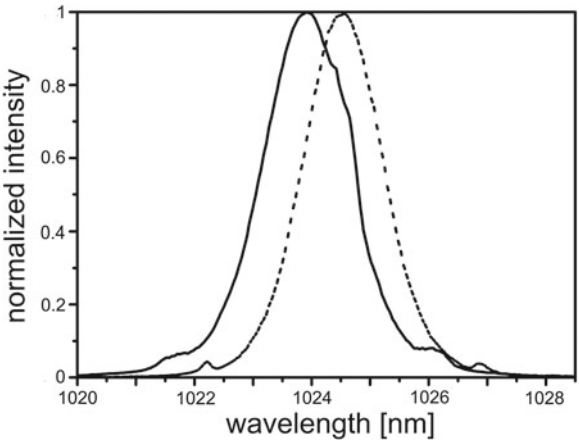

Fig. 1.4 Oscillator output spectrum with air (*black solid*) and helium (*black dotted*)

equals 2.34 W at 1 MHz repetition rate leading to pulse energies of 2.34 μJ in combination with nearly Fourier limited pulse durations of about 700 fs. Figure 1.4 shows the corresponding spectrum (solid line). To minimize the nonlinearities from the ambient air, the resonator laserbox is purged with helium in a second step. Here, stable operation with more than 3 μJ of pulse energy and durations of 680 fs have been obtained (spectrum in Fig. 1.4, dashed line).

Compared to the bulk concept, two main drawbacks of the thin-disk concept with cavity-dumping can be pointed out. On the one hand side, the dumping ratios are relatively low (∼25 % in contrast to more than 50 % in the bulk concept). As a reason for this, the low single pass gain is found to be the main limitation (see Sect. 1.1.4). Supplementary the pulse duration is relatively long (∼700 fs) compared to 400 fs in the bulk setup. Here, etalon and hole-burning effects lead to unstable operation for bandwidths larger than 1.8 nm [10]. Thus, the available gain bandwidth has to be restricted by means of a birefringent filter (BRF) inside the cavity.

1.1.4 Limits of Cavity-Dumping in Thin-Disk Oscillators

The maximum achievable peak power from the oscillator is limited by the B-Integral in the cavity. By using Yb:YAG thin-disk modules this limitation can be overcome and pulse energies up to 11 μJ at a repetition rate of 4 MHz have been demonstrated in SESAM mode-locked oscillators with pulse durations of 790 fs [11]. As elaborated in Sect. 1.1.3 the thin-disk oscillator with cavity-dumping based on Yb:KYW resulted in pulse energies up to 3 μJ at a repetition rate of 1 MHz with pulse durations of 680 fs [1]. Currently, the limiting factor for the pulse energy in this setup is the dumping ratio which, at 24 %, is far lower than in the previous

experiments with bulk material (see Sect. 1.1.1) where the maximum dumping ratio easily exceeds 50 %.

To understand the reasons for this limitation and to find ways of improving the performance of our laser we started to investigate the theoretical properties of such laser systems. In this section we present a theoretical study of cavity-dumped systems with special regard to how the implementation of a thin-disk scheme affects the dynamic properties of the cavity-dumped laser. The comparison between the numerical model and experiments allows for determining inherent limits of the current setups and finding possible ways for improvement.

It is possible to accurately describe the dynamics of a SESAM mode-locked laser by using three differential equations which describe the temporal dynamics of the pulse envelope, the laser gain and the absorber loss. The detailed equations and parameters are given in [12]. The excellent agreement between numerical simulations and experimental data forms the basis for the theoretical investigation of the limiting factors for cavity-dumping. From this treatment we expect a deeper understanding of the pulse shaping mechanisms and some guidelines how to extract some higher fraction of the intracavity pulse energy. Not surprisingly, the numerical model revealed the same limitation for the maximum dumping ratio for the thin-disk setup between 25 and 30 % with the parameter sets close to the experimental values. Higher dumping ratios result in Q-switching instabilities, and no stable cw mode-locked laser operation was possible. Nevertheless, the question is, what is the reason for the big difference in the maximum dumping ratio between the bulk and thin-disk setup? Looking at the two laser setups, the main difference in terms of the gain dynamics is the mode radius in the gain medium. While the mode radius in an Ytterbium bulk laser is typically around 100 µm, the same parameter in a thin-disk setup is typically more than 5 times larger. Indeed Fig. 1.5 reveals that the key factor for the stability of a cavity-dumped mode-locked laser is the mode size in the gain medium.

In the simulations we varied the mode radius from 540 µm down to 200 µm. Starting from a plateau at around 18 % for large mode radii the stability border grows linearly to above 80 % as the mode radius is reduced. It is also important to note that the small signal gain was kept constant while the mode size was scanned. In the experiment this is only possible up to a certain point because the small signal gain is directly linked to the pump power and the pump power density is limited by saturation effects in the gain medium and the damage threshold of the disk. With our used disk the maximum pump power density is limited to 4 kW/cm^2 which would be reached at a mode radius of 350 µm. So for even smaller pump radii the pump power would have to be decreased which would still allow for an increased dumping ratio but at the expense of a reduction in pulse energy. In the more realistic scenario, starting with the parameters of the thin-disk laser and continuously reducing both pump power and laser mode area on the disk one eventually ends up with a system very similar to the bulk laser described in Sect. 1.1.1. At this end the maximum dumping ratio could easily exceed 50 % but the pulse energy would be decreased to about 1 µJ. In a qualitative sense the importance of the mode size can be understood simply by analyzing its influence on the small signal gain and the

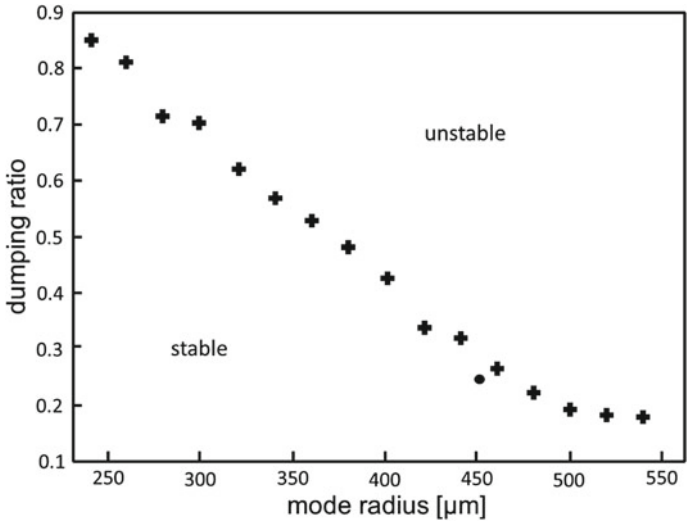

Fig. 1.5 Calculated maximum dumping ratio for stable cw mode-locking operation in the thin-disk laser as a function of the beam radius on the laser disk. The *black dot* marks the parameters of the experiment from Sect. 1.1.3

saturation energy of the laser. A larger mode radius on the disk leads to an increase in saturation energy at the expense of a smaller gain. As described by Hönninger et al. [13] the pulse energy E_p necessary to avoid Q-switching in a SESAM mode-locked laser without cavity-dumping can be calculated using the following equation

$$E_p^2 > E_{sat,A} E_{sat,L} \Delta R, \tag{1.1}$$

where ΔR is the SESAM reflectivity modulation depth, $E_{sat,A}$ is the saturation energy of the absorber, and $E_{sat,L}$ that of the laser gain medium. Here, an increase in the saturation energy of the laser will result in an increased threshold for stable cw mode-locked operation. For a thin-disk laser like the one described in [11] this is of little consequence since the low output coupling ratio ensures that the intracavity pulse energy is usually high enough to avoid Q-switching instabilities. In the case of a cavity-dumped laser however the situation is different, since the small-signal stability analysis behind (1.1) is not valid anymore. From our model the numerical value for the threshold was found to be up to an order of magnitude higher in the case of a cavity-dumped laser.

Still (1.1) provides a good starting point for a systematic investigation of the cavity-dumped thin-disk oscillator. We started by varying two key parameters of the model, the mode area on the gain medium and the modulation depth of the SESAM. The left part of Fig. 1.6 shows the maximum dumping ratio for different modulation depths ΔR and different mode radii r_{gain} color coded between blue and red. It can be seen that, in accordance with the discussion of (1.1), higher

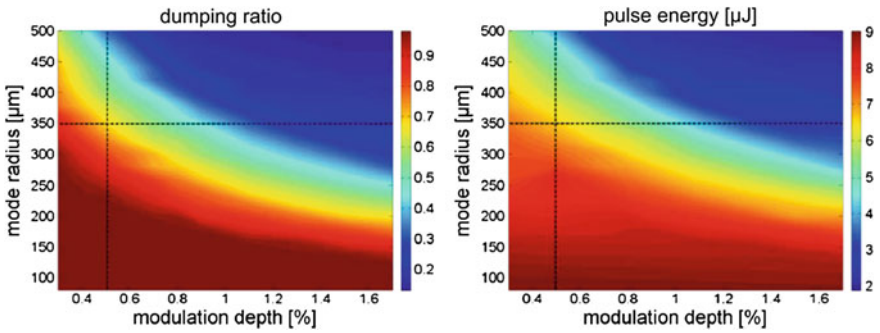

Fig. 1.6 *Left* Maximum dumping ratio as a function of the mode radius on the disk and the modulation depth of the SESAM. *Red color* denotes a high ratio, *blue color* a low ratio. *Right* Resulting out-coupled pulse energies in µJ for the same set of parameters. *Red color* denotes high energy, *blue color* low energy. The *dashed lines* indicate experimental limits. The maximum power density, i.e. the minimal mode radius on the disk (*horizontal*) and the minimal modulation depth for stable mode-locking (*vertical*) leave only the *upper right* quadrant experimentally accessible

modulation depths lead to lower possible dumping ratios. But nevertheless even for small modulation depths the mode radius is still the dominant parameter. For modulation depths exceeding 1.5 % the maximum dumping ratio depends almost exclusively on the mode radius.

The right part of Fig. 1.6 shows the maximum stable pulse energy in units of µJ that would be coupled out with the dumping ratios shown in the left. The dashed lines indicate some empirical experimental limitations: The vertical line stems from the fact that for modulation depths lower than 0.5 % only cw operation of the laser was possible as the loss modulation was not high enough to achieve stable mode-locking. The horizontal line represents the power density damage limit of the Yb:KYW disk of 4 kW/cm^2. So the accessible regime is limited to the upper right quadrant in the two plots. By choosing optimum parameters pulse energies around 6 µJ should be achievable. It also needs to be pointed out that even if the limitation of the power density on the disk could be overcome, any substantial increase in pump power would lead to other problems. To fulfill the soliton condition in our cavity-dumped oscillator (which is currently done by using home designed chirped mirrors) we need to accumulate a second order dispersion (GDD) of −40,000 fs^2. Since any increase in intracavity power results in an increase in the nonlinearities in the cavity, even larger values of the GDD would be required for compensation, which might be hard to achieve by mirrors. One solution could be laser operation in the positive dispersion regime (see Sect. 1.1.2).

The third variable given in (1.1) is the saturation energy of the absorber which forms a third accessible degree of freedom. Unfortunately, in the experiment it has been found that the mode size on the SESAM is limited to a very narrow range roughly between 270 and 450 µm. For smaller mode radii the SESAM is prone to damage because of the high intensities, while for larger radii no stable cw-mode locking was possible. For this reason the mode area on the SESAM does not seem

to offer a large potential for optimizing the maximum output pulse energy of the mode-locked thin-disk laser.

In conclusion, the obvious way to optimize the dumping performance is to increase the small-signal gain by reducing the beam diameter or by increasing the pump power. This is easiest realizable in an oscillator with two bulk gain crystals, which will be elaborated in the next section. However, the thin-disk concept is well-suited for the regenerative amplification concept as discussed in Sect. 1.2.

1.1.5 Chirped-Pulse Oscillator with Two Yb:KYW Bulk Crystals

As discussed in Sect. 1.1.4 energy scaling concerning cavity-dumped systems is restricted to bulk-based laser technology since the thin-disk scheme does not allow for sufficient dumping efficiencies. For higher energies it is necessary to increase the pump power. However a single bulk-crystal laser is limited in terms of both applicable pump power and thermal load. For instance when applying pump powers of more than 30 W to pump diameters of 300 µm the laser clearly exhibits anisotropic beam distortion and a strong tendency to transversal multi-mode operation. Especially the anisotropic properties of the Yb:KYW crystal lead to asym-metric effects such as elliptical beam profiles and astigmatism, respectively. In the worst case the crystal will break under the thermal load. In order to prevent the gain medium from such events the pump power can be divided onto two or even more crystals. In that way higher pump power levels become possible. Moreover this approach allows for a higher net-gain which is ideal to reach high cavity-dumping efficiencies.

For such an oscillator the laser setup equals the previous bulk-laser configuration (see Fig. 1.1) except that there are two separate Yb:KYW-crystals each pumped by a fiber coupled laser diode at 981 nm (Fig. 1.7) [14]. With a total absorbed pump power of almost 20 W this system reaches pulse energies of 7 µJ (average power: 7 W) at 1 MHz dumping frequency. At this point the maximum dumping efficiency is around 67 % which is—as expected—even better than for the single-bulk-laser.

With respect to the power values the oscillator works with an optical-to-optical efficiency of almost 20 % which is outstanding for mode-locked oscillators with cavity-dumping. The net GDD is at +3500 fs^2 where mode-locking is the most stable over the widest pulse energy range. The GDD can be altered by varying the amount of negative dispersive mirrors (GTI). The Gaussian shaped chirped pulses inside the resonator feature FWHM-durations of 14 ps.

The power spectrum is displayed in Fig. 1.8. Calculating the Fourier-limit from the spectrum yields a pulse duration of 261 fs. Low-loss pulse compression into the femtosecond regime can be realized by means of the compressor setup from Fig. 1.7.

This compact configuration uses one transmission grating (here: 1250 lines/mm) and gives rise to losses below 13 %. This compressor allowed for measured pulse durations as short as 416 fs at the best compressor alignment. With respect to the

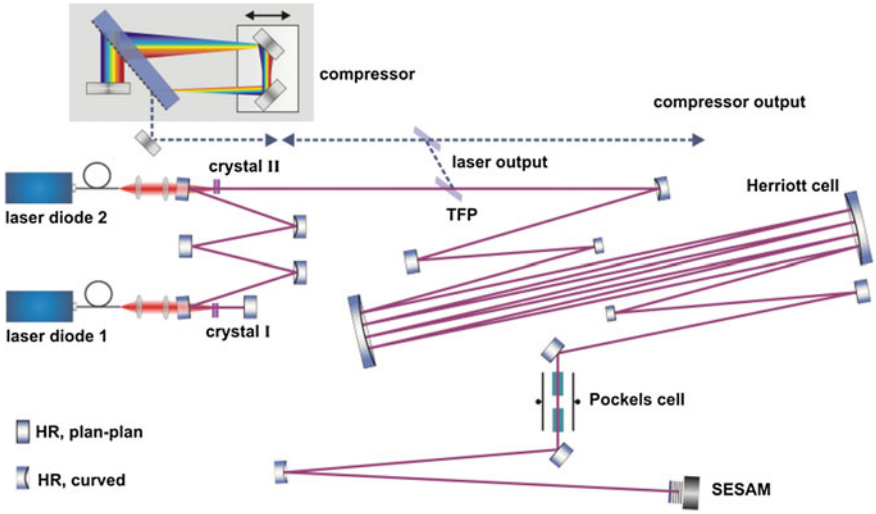

Fig. 1.7 Schematic of the two-crystal laser and the external compressor

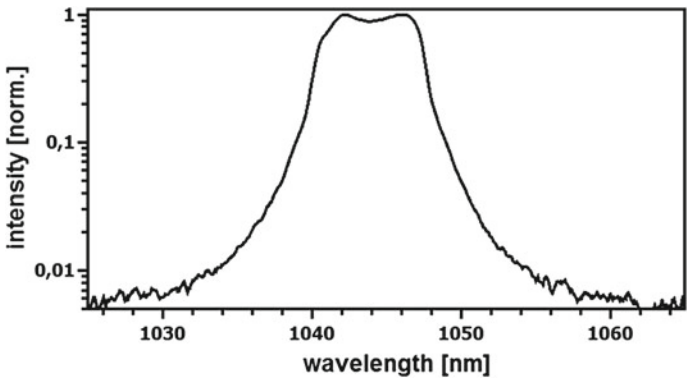

Fig. 1.8 Power spectrum of the two-crystal bulk laser

investigated system the Fourier-limited pulse duration could not be reached due to higher order dispersion. The residual third order dispersion (TOD) from the grating was calculated to be around +0.007 ps^3. By means of calculations and dispersion measurements one resonator mirror could be identified as a further high TOD-source where a TOD of +0.017 ps^3 was accumulated. Nonetheless pulse energies of 6.1 µJ were measured behind the compressor yielding a total peak power of 12 MW. Apart from the pulse properties very good power noise properties (rms < 1 %) and beam characteristics (M^2: 1.1) have been observed. This is due to the compact setup (0.9 × 0.5 × 0.3 m) and the sealed laser box.

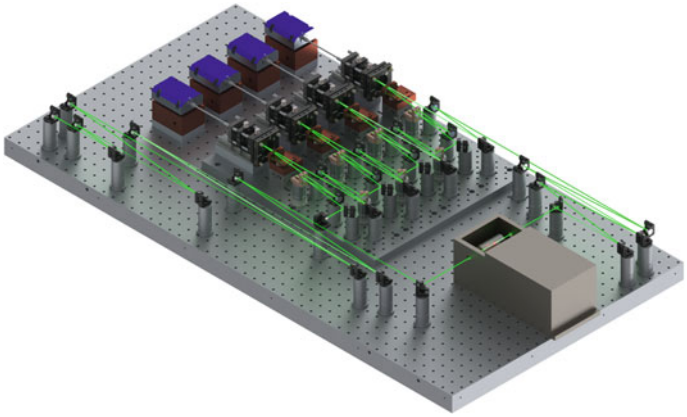

Fig. 1.9 Schematic picture of a four-crystal bulk-laser with cavity dumping

Current and future research will account for even higher energies implying more than two crystals at higher pump power levels. As part of this work no particular energy scaling limitation could be found and multi-crystal approaches seem feasible (see principle setup illustrated in Fig. 1.9). There are also intentions to further decrease the available pulse duration. As an optimized TOD-management would most likely improve the presented system other concepts deal with the combination of different gain spectra.

The fundamental idea is to operate the oscillator under different gain spectra simultaneously (i.e. the N_p-, and N_m-spectrum in Yb:KYW) to enhance the spectral width of the pulses and in turn to generate shorter pulse durations. However, recent experiments indicate that the combination of the different gain spectra within the resonator is cannot be stabilized. The laser dynamics prefers one of the gain spectra and the other one is suppressed. Nevertheless, this concept works well with amplifiers [15] (see also Sect. 1.2).

1.1.6 Applications

The laser systems described before have been employed in some selected applications such as waveguide writing, two-photon polymerization or as seed sources for different amplification procedures.

1.1.6.1 Waveguide Writing

With the pulses of the contemplated lasers a straightforward fabrication of optical waveguides in transparent materials is possible. When these pulses are tightly focussed inside a bulk material, the intensity in the focal volume becomes high

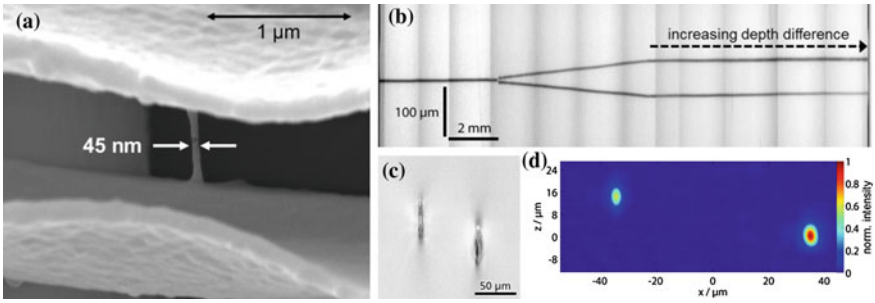

Fig. 1.10 **a** SEM images of a free hanging 2PP line structure [18]. **b** Simultaneously written 3D Y-Splitter with linearly increasing depth difference on the right half. **c** Cross-sectional microscope views of the end faces of the 3D coupler, the depth difference at the end is 13.8 µm. **d** Near field profiles of the output beams [19]

enough to cause absorption through nonlinear processes. This leads to a localized, permanent refractive index change, allowing direct fabrication of guiding structures. Unlike systems with lower repetition rates, femtosecond laser writing with 1 MHz repetition rate in general gives rise to thermal diffusion and heat accumulation effects which lead to an increase in the waveguide diameter and an increase in the refractive index contrast, while reducing the waveguide losses.

Fused silica is a common material for waveguide writing; Although we did not observe heat accumulation here with the laser parameters available, a significant refractive index increase has been achieved, which is high enough to produce multiple parallel waveguides, complex couplers [16], and 3D splitters in a single sweep (see Fig. 1.10b–d) [17]. These structures provide single mode guiding and variable coupling/splitting ratios for light at 976 and 1550 nm. Using special beam shaping methods various photonic devices are easily achievable just by software control for complex but flexible 3D photonic networks, e.g. for optical sensing in lab-on-a-chip devices.

1.1.6.2 Two-Photon Polymerization (2PP)

The two-photon polymerization (2PP) process involves temporal as well as spatial overlap of photons, resulting in a nonlinear absorption in a highly localized volume. The absorbed photons induce chemical reactions between starter molecules and monomers within the medium, inducing the polymerization. Using liquid materials polymerization results in localized solidification of the fluid.

Since the region for the light/matter interaction is limited within the focal volume one can fabricate any computer-generated 3D structure, by producing a trace of polymerized material, if the laser focus moves within such photosensitive material. Because of a quadratic intensity dependence of the two-photon-absorption probability and the well-defined polymerization threshold resolutions of less than 50 nm in the fabricated structures can be reached [20, 21] (see Fig. 1.10a). Direct laser-

writing of dielectric-loaded surface plasmon–polariton wave-guides (DLSPPWs) for the visible and near infrared is one possible application of 2PP [19]. Such structures can also be used for realizing masters for nanoimprint techniques to produce DLSPPWs [18, 22].

1.1.6.3 Seed Oscillators for Amplifier Systems (Fiber Amplifier, OPA/NOPA)

The transfer from new laser technology into the application laboratories is well established. Laser systems like the above mentioned are ideal seed sources for miscellaneous amplifier applications. With the oscillator discussed in Sect. 1.1.1 it was possible to pump an optical parametric amplifier (OPA) directly by a femtosecond oscillator first time [23]. Wavelength-tunable pulses in the signal—(0.65–0.85 μm) and idler range (1.4–2.5 μm) are generated at a repetition frequency of 1 MHz. Pulses with 30 nJ of energy and a duration of 16 fs are achieved from a super-continuum seed generated in a sapphire plate.

Many different applications in physics, chemistry, biology, and medicine profit from ultrafast lasers with high pulse energies, from lasers with short pulses, and from lasers with high pulse repetition rates. The literature is full of reports on lasers which can fulfill one or two of the desired requirements. But some applications such as nonlinear bio-imaging or spectroscopy need them simultaneously, and here one laser system which is capable of meeting all three goals simultaneously was demonstrated: a noncollinear optical parametric amplifier pumped by a MHz/μJ-oscillator with cavity-dumping (MHz-NOPA) [24]. This system can produce few-cycle pulses with MHz repetition rates and pulse energies/peak powers well beyond the typical oscillator level. Finally, it could be easily scaled with the occurred progress in pump laser technology. In particular, the single-stage amplification of a cavity-dumped Yb:KYW laser oscillator with a Yb-doped rod-type fiber allows the generation of 420 fs pulses with a pulse energy of 9 μJ at a1 MHz repetition rate [25]. Driven by these pulses a noncollinear optical parametric amplifier (NOPA) delivering sub 10 fs pulses with 420 nJ of pulse energy was realized [26]. The ultra-broadband seed used for this system is based on stable white-light generation from the 420 fs long pulses in a Yttrium aluminium garnet (YAG) plate.

1.2 Regenerative Amplification with Yb:KYW and Yb:KLuW Thin-Disks

In Sect. 1.1.4 it has been elaborated that the thin-disk concept is limited for use in cavity-dumped oscillators. However, it is well-suited for the amplification of short pulses. For gain media with low single pass gain, a multi pass configuration is necessary to achieve high amplification factors. The most flexible multi pass

amplifier setup is a regenerative amplifier. In principle regenerative amplification is divided in two periods in the temporal domain. In a first period the amplifier is pumped without seeding. This regeneration period is followed by an amplification period, where a single seed pulse is switched in and out of the amplifier.

Placing the amplifying medium in an optical resonator offers the possibility for multiple amplifier cavity roundtrips. In this way, the gain factor can easily be controlled by the number of cavity roundtrips and very high amplification factors can be achieved. The switching unit can be realized by an electro-optic modulator (EOM) in combination with a polarizer. As seed pulses usually ps and fs pulses are used. In general laser crystals for such setups are cuboids and thin-disks [27].

The thin-disk geometry offers the well-known possibility to decrease the intensity by scaling the spot size on the disc. Furthermore, the efficient thermal management of thin-disks makes them the most promising candidates for high power amplifiers. Especially in ultra-short pulse operation, thin-disk regenerative amplifiers (RA) emitting at 1 µm are convenient tools for a variety of applications like micromachining and waveguide writing in transparent media (see also Sect. 1.1.6).

However, less work has been done in the development of RA emitting dechirped pulse durations below 200 fs. The main challenge to achieve such short pulse durations is to overcome the gain narrowing effect, i.e. the spectral narrowing during amplification due to the spectral gain profile [28]. Several techniques are used to balance the spectral narrowing, such as spatially dispersive amplification [29], regenerative spatial shaping by intracavity elements [30] and seed pulse shaping in phase and amplitude [31, 32].

Another simple method to balance gain narrowing is to use different gain media to achieve a broad effective gain bandwidth. In particular for biaxial crystals the effective gain bandwidth can easily be increased by amplifying the pulses with polarization parallel to the different optical axes. In the wavelength region of 1 µm potassium yttrium and lutetium monoclinic double tungstate oxide (Yb:$KY(WO_4)_2$, Yb:$KLu(WO_4)_2$) are promising candidates for ultra-short pulsed regenerative amplifiers with and without gain combining [15, 33].

A chirped pulse amplifier was set up consisting of an ytterbium fiber based ultra-short pulse oscillator, a fiber based stretcher and pre-amplifier, a RA based on a Yb:$KY(WO_4)_2$ and a Yb:$KLu(WO_4)_2$ thin-disk and a GRISM (Grating-Prism) compressor. For the experiments where the Yb:KYW thin-disk was used as gain medium, the output pulses of the pre-amplifier had a central wavelength of 1034 nm, a pulse duration of 31 ps and a pulse energy of 9 nJ. The pulses of the seed oscillator could be dechirped to the Fourier limited pulse duration of 152 fs by using the GRISM compressor.

The designed RA setup, shown in Fig. 1.11, allowed 12 passes through the thin-disk per cavity roundtrip. Gain combining was done in every single roundtrip by rotating the polarization through 90°. Thus, the amplifying optical axis was changed between N_p and N_m. The thin-disk had an Yb concentration of 10 at.%, a diameter of 7 mm and a thickness of 102 µm. As pump source a laser diode was used, which had a wavelength of 981 nm and a maximum pump power of 78 W.

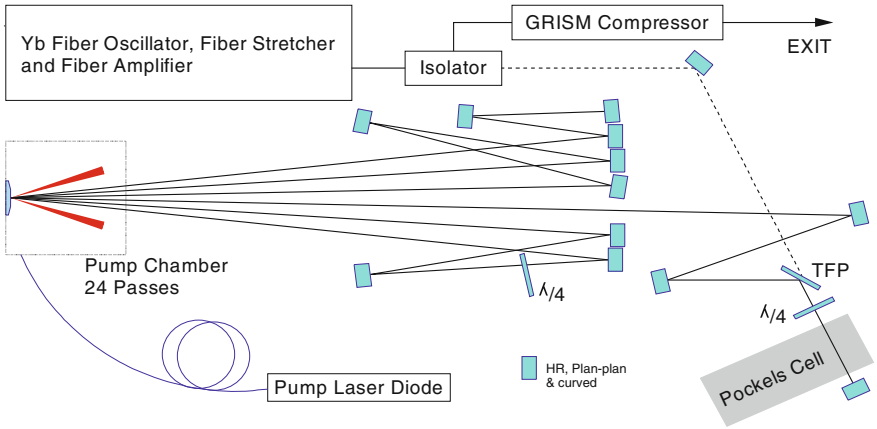

Fig. 1.11 Setup of the thin-disk based regenerative amplifier system

A Pockels-cell consisting of two β-barium borate crystals (BBO) together with a thin-film polarizer served as electro optical switch, which allowed repetition rates up to 200 kHz. The thin-disk was placed in a pump chamber consisting of a collimator for the pump diode fiber and a parabolic mirror, which enabled 24 passes of the pump beam through the thin-disk. The outcoupled pulses were dechirped with a GRISM compressor, which consisted of a grating and a prism and enabled a simultaneous compensation of second- and third order dispersion [34].

The RA was operated at a repetition rate of 20 kHz. The output pulse energy of the amplifier was easily scaled by increasing the number of cavity roundtrips. A variation between 38 and 53 roundtrips resulted in a pulse energy change from 114 to 500 μJ, measured behind the GRISM compressor. The optical spectrum of the output pulses at pulse energies of 500 μJ is shown at the left side in Fig. 1.12. A bandwidth of 9.3 nm and a central wavelength of 1031 nm were calculated by the second moment normalized to the FWHM of a Gaussian shape. The spectral modulation indicates a satellite pulse, which had its origin in an etalon between the surfaces of the half wave plate in the resonator. From the optical spectrum we calculated a Fourier limited pulse duration of 185 fs. The corresponding autocorrelation trace is shown on the right side of Fig. 1.12. It has a FWHM of 268 fs corresponding to a pulse duration of 185 fs, which is the Fourier limited pulse duration.

In a second experiment an Yb:KLuW thin-disk was used in a similar setup without polarization rotation [35]. For this experiment, the seed pulses had a pulse energy of 4 nJ, a pulse duration of 43 ps and a dechirped pulse duration of 170 fs. The central wavelength of the seed pulses was 1026 nm and was matched to the emission maximum of the thin-disk.

The output pulse energy of the amplifier was again scaled by increasing the roundtrip number. A variation from 28 to 44 cavity roundtrips resulted in a pulse energy change from 50 μJ to a maximum of 400 μJ. The pulse durations were

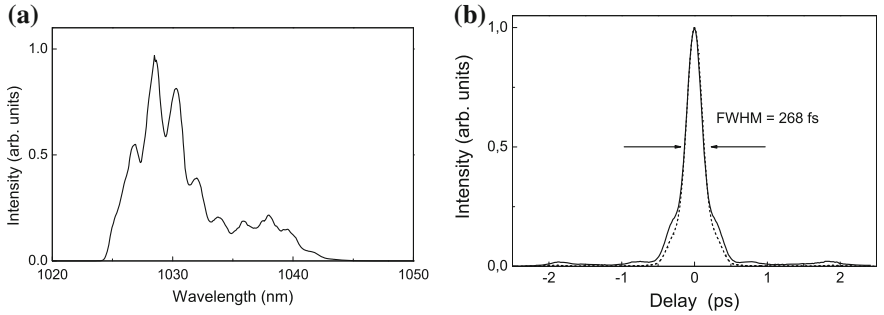

Fig. 1.12 Optical spectrum of the output pulses (*left*) and corresponding autocorrelation (*right*) at a pulse energy of 500 µJ

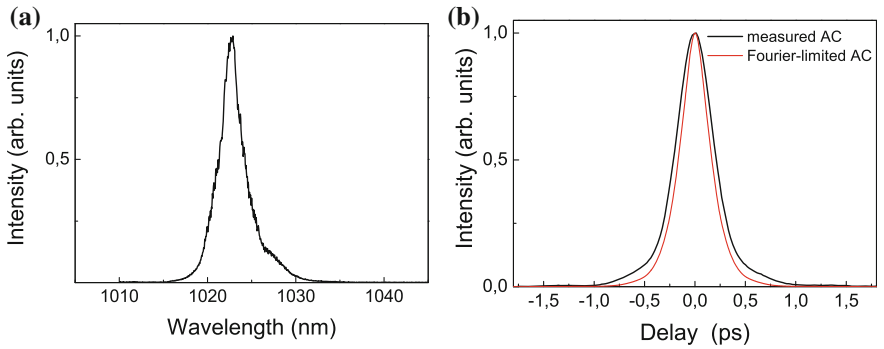

Fig. 1.13 Power spectrum (*left*) and the autocorrelation function together with Fourier limited autocorrelation (*right*) at the maximum pulse energy

nearly independent from the roundtrip number and remained between 190 and 214 fs. The power spectrum and the autocorrelation function at the maximum pulse energy are depicted in Fig. 1.13. The spectral FWHM was 2.9 nm and the central wavelength 1022.7 nm while the autocorrelation trace had a FWHM of 426 fs. A deconvolution factor of 2.16 was calculated, resulting in a pulse duration of 197 fs, which is 21 % above the Fourier-limit. Additionally, the measurement of pulse durations at different repetition rates between 20 and 125 kHz at constant pump power level yielded nearly similar values around 210 fs.

These results revealed the ability of operating the developed RA at different round trip numbers as well as at different repetition rates without a significant change of the dechirped pulse durations.

In conclusion ultrafast thin-disk regenerative amplifiers were demonstrated with the active media Yb:KYW and Yb:KLuW. In the case of Yb:KYW, a pulse duration below 200 fs was achieved at a pulse energy of 500 µJ. A regenerative thin-disk amplifier based on Yb:KLuW was demonstrated for the first time, delivering a pulse energy of 400 µJ at a pulse duration of 197 fs.

1.3 Conclusion

In this chapter results on Yb-based cavity-dumped solid state oscillators and regenerative amplifiers supplemented by some selected applications were presented.

In the case of cavity-dumped oscillators it has been shown that the thin-disk concept is not well suited compared to bulk lasers because of the limited dumping ratio. Nevertheless 790 fs pulses with energies of 3 μJ at 1 MHz could be achieved from an Yb:KYW thin-disk oscillator. Due to the usage of a two crystal Yb:KYW setup in combination with the CPO concept an increase in the already high dumping ratio of the bulk material could be obtained ending up in 7 μJ of pulse energy at 1 MHz repetition rate and a compressed pulse duration of 416 fs.

For the presented regenerative amplifiers Yb:KYW and Yb:KLuW thin-disks were used as gain media. By gain combining of the axes N_m and N_p a dechirped pulse duration of 185 fs was achieved at a pulse energy of 500 μJ for the Yb:KYW thin-disk. Another regenerative amplifier was demonstrated for the first time based on a an Yb:KLuW thin-disk, resulting in dechirped pulse durations below 200 fs at a pulse energy of 400 μJ.

References

1. G. Palmer, M. Siegel, A. Steinmann, U. Morgner, Opt. Lett. **32**(11), 1593 (2007). doi: 10.1364/OL.32.001593. http://ol.osa.org/abstract.cfm?URI=ol-32-11-1593
2. A. Killi, A. Steinmann, J. Dörring, U. Morgner, M.J. Lederer, D. Kopf, C. Fallnich, Opt. Lett. **30**(14), 1891 (2005). doi:10.1364/OL.30.001891. http://ol.osa.org/abstract.cfm?URI=ol-30-14-1891
3. S.M.J. Kelly, **28**, 806 (1992). doi: 10.1049/el:19920508. http://ieeexplore.ieee.org/stamp/stamp.jsp?tp=&arnumber=133147&isnumber=3651
4. N.J. Smith, K.J. Blow, I. Andonovic, **10**, 1329 (1992). doi:10.1109/50.166771.ieeexplore.ieee.org/xpls/abs_all.jsp?arnumber=166771&tag=1
5. A. Killi, U. Morgner, **12**(15), 3397 (2004). http://www.opticsexpress.org/abstract.cfm?URI=oe-12-15-3397
6. G. Palmer, M. Emons, M. Siegel, A. Steinmann, M. Schultze, M. Lederer, U. Morgner, Opt. Express **15**(24), 16017 (2007). doi:10.1364/OE.15.016017. http://www.opticsinfobase.org/abstract.cfm?URI=oe-15-24-16017
7. A. Giesen, in *Proceedings of SPIE*, vol. 5332 (2004), pp. 212–227. doi:10.1117/12.547973. http://spie.org/x648.html?product_id=547973
8. A. Giesen, in *European Symposium on Optics and Photonics for Defence and Security* (International Society for Optics and Photonics, 2004), pp. 112–127. doi:10.1117/12.578272. http://proceedings.spiedigitallibrary.org/proceeding.aspx?articleid=853172
9. TGSW Stuttgart, http://tgsw-photonics.de/scheibenlasertechnologie. http://tgsw-photonics.de/scheibenlasertechnologie
10. R. Paschotta, J.A. der Au, G.J. Spühler, S. Erhard, A. Giesen, U. Keller, **B 72**, 267 (2001). doi:10.1007/s003400100486. http://link.springer.com/article/10.1007%2Fs003400100486?LI=true
11. S.V. Marchese, C.R. Baer, A.G. Engqvist, S. Hashimoto, D.J. Maas, M. Golling, T. Südmeyer, U. Keller, **16**(9), 6397 (2008). http://www.opticsexpress.org/abstract.cfm?URI=oe-16-9-6397

12. M. Siegel, G. Palmer, A. Steinmann, M. Pospiech, U. Morgner, **15**(25), 16860 (2007). doi:10.1364/OE.15.016860. http://www.opticsexpress.org/abstract.cfm?URI=oe-15-25-16860
13. C. Hönninger, R. Paschotta, F. Morier-Genoud, M. Moser, U. Keller, **B 16**, 46 (1999). doi:10.1364/JOSAB.16.000046. http://www.opticsinfobase.org/josab/abstract.cfm?id=35627
14. G. Palmer, M. Schultze, M. Emons, A.L. Lindemann, M. Pospiech, D. Steingrube, M. Lederer, U. Morgner, **18**(18), 19095 (2010). doi:10.1364/OE.18.019095. http://www.opticsexpress.org/abstract.cfm?URI=oe-18-18-19095
15. U. Buenting, H. Sayinc, D. Wandt, U. Morgner, D. Kracht, **17**, 8046 (2009). doi:10.1364/OE.17.008046. http://www.opticsinfobase.org/oe/abstract.cfm?uri=oe-17-10-8046
16. M. Pospiech, M. Emons, A. Steinmann, G. Palmer, R. Osellame, N. Bellini, G. Cerullo, U. Morgner, **17**(5), 3555 (2009). http://www.opticsexpress.org/abstract.cfm?URI=oe-17-5-3555
17. M. Pospiech, M. Emons, B. Väckenstedt, G. Palmer, U. Morgner, **18**(7), 6994 (2010). doi:10.1364/OE.18.006994. http://www.opticsexpress.org/abstract.cfm?URI=oe-18-7-6994
18. A. Seidel, C. Reinhardt, T. Holmgaard, W. Cheng, T. Rosenzveig, K. Leosson, S. Bozhevolnyi, B. Chichkov, IEEE Photonics J. **2**(4), 652 (2010). doi:10.1109/JPHOT.2010.2056490. http://ieeexplore.ieee.org/xpls/abs_all.jsp?arnumber=5512549&tag=1
19. C. Reinhardt, A. Seidel, A. Evlyukhin, W. Cheng, R. Kiyan, B. Chichkov, Appl. Phys. A: Mater. Sci. Process. **100**(2), 347 (2010). doi:10.1007/s00339-010-5872-0. http://link.springer.com/article/10.1007%2Fs00339-010-5872-0?LI=true#page-1
20. M. Emons, K. Obata, T. Binhammer, A. Ovsianikov, B.N. Chichkov, U. Morgner, Opt. Mater. Express **2**(7), 942 (2012). doi:10.1364/OME.2.000942. http://www.opticsinfobase.org/ome/abstract.cfm?URI=ome-2-7-942
21. V. Paz, M. Emons, K. Obata, A. Ovsianikov, S. Peterhänsel, K. Frenner, C. Reinhardt, B. Chichkov, U. Morgner, W. Osten, J. Laser Appl. **24**(4), 042004 (2012). doi:10.2351/1.4712151. http://jla.aip.org/resource/1/jlapen/v24/i4/p042004_s1
22. A. Seidel, C. Ohrt, S. Passinger, C. Reinhardt, R. Kiyan, B.N. Chichkov, J. Opt. Soc. Am. B **26**(4), 810 (2009). doi:10.1364/JOSAB.26.000810. http://josab.osa.org/abstract.cfm?URI=josab-26-4-810
23. A. Killi, A. Steinmann, G. Palmer, U. Morgner, H. Bartelt, J. Kobelke, Opt. Lett. **31**(1), 125 (2006). doi:10.1364/OL.31.000125. http://ol.osa.org/abstract.cfm?URI=ol-31-1-125
24. A. Steinmann, A. Killi, G. Palmer, T. Binhammer, U. Morgner, Opt. Express **14**(22), 10627 (2006). doi:10.1364/OE.14.010627. http://www.opticsexpress.org/abstract.cfm?URI=oe-14-22-10627
25. A. Steinmann, G. Palmer, M. Emons, M. Siegel, U. Morgner, Laser Phys. **18**, 527 (2008). doi:10.1134/S1054660X08050010. http://dx.doi.org/10.1134/S1054660X08050010
26. M. Emons, A. Steinmann, T. Binhammer, G. Palmer, M. Schultze, U. Morgner, Opt. Express **18**(2), 1191 (2010). doi:10.1364/OE.18.001191. http://www.opticsexpress.org/abstract.cfm?URI=oe-18-2-1191
27. C. Hönninger, I. Johannsen, M. Moser, G. Zhang, A. Giesen, U. Keller, Appl. Phys. B **65**, 423 (1997). doi:10.1007/s003400050291
28. P. Raybaut, F. Balembois, F. Druon, P. Georges, IEEE J. Quantum Electron. **41**(3), 415 (2005). doi:10.1109/JQE.2004.841930. http://ieeexplore.ieee.org/xpls/abs_all.jsp?arnumber=1397888
29. N.B. Chichkov, U. Bünting, D. Wandt, U. Morgner, J. Neumann, D. Kracht, Opt. Express **17**(26), 24075 (2009). doi:10.1364/OE.17.024075. http://www.opticsexpress.org/abstract.cfm?URI=oe-17-26-24075
30. C.P.J. Barty, G. Korn, F. Raksi, C. Rose-Petruck, J. Squier, A.C. Tien, K.R. Wilson, V.V. Yakovlev, K. Yamakawa, Opt. Lett. **21**(3), 219 (1996). doi:10.1364/OL.21.000219. http://ol.osa.org/abstract.cfm?URI=ol-21-3-219
31. C.W. Hillegas, J.X. Tull, D. Goswami, D. Strickland, W.S. Warren, Opt. Lett. **19**(10), 737 (1994). doi:10.1364/OL.19.000737. http://ol.osa.org/abstract.cfm?URI=ol-19-10-737
32. A. Monmayrant, B. Chatel, Rev. Sci. Instrum. **75**(8), 2668 (2004). doi:10.1063/1.1771492. http://ieeexplore.ieee.org/xpl/freeabs_all.jsp?arnumber=5001085&abstractAccess=no&userType=inst

33. A. Buettner, U. Buenting, D. Wandt, J. Neumann, D. Kracht, Opt. Express **18**(21), 21973 (2010). doi:10.1364/OE.18.021973. http://www.opticsexpress.org/abstract.cfm?URI=oe-18-21-21973
34. S. Kane, J. Squier, J. Opt. Soc. Am. B **14**(3), 661 (1997). doi:10.1364/JOSAB.14.000661. http://josab.osa.org/abstract.cfm?URI=josab-14-3-661
35. H. Sayinc, U. Buenting, D. Wandt, J. Neumann, D. Kracht, Opt. Express **17**(17), 15068 (2009). doi:10.1364/OE.17.015068. http://www.opticsexpress.org/abstract.cfm?URI=oe-17-17-15068

http://www.springer.com/978-3-319-17658-1

Ultrashort Pulse Laser Technology
Laser Sources and Applications
Nolte, S.; Schrempel, F.; Dausinger, F. (Eds.)
2016, XVIII, 358 p., Hardcover
ISBN: 978-3-319-17658-1